

THE COMPLEX STIFFNESS METHOD OF DAMPING FOR CONSTRAINED DAMPING STRUCTURE WITH A STAND-OFF LAYER

Wenjun ZHANG¹, Dagang SUN², Bijuan YAN³, Zhanlong LI⁴

The stand-off layer can add the distance between the base layer and the damping layer and can increase the deformation of damping layer which enables the constrained damping structure with a stand-off layer (CDSWASL) to have a better damping effect than that of traditional constrained damping structure (TCDS). In this paper, the loss factor of (CDSWASL) is induced through the complex stiffness method (CSM), and is verified by FEM. The comparisons and contrasts of loss behavior are made between TCDS and CDSWASL for a cantilever damping beams to demonstrate that CDSWASL can exert a better damping effect than that of TCDS of the same size. At last, the effects of thickness and material of stand-off layer on loss factor of the structure are discussed: the thicker the stand-off layer is, the better CDSWASL damping effect will be; when the ratio of elastic modulus $E_2/E_3=1000$, the best damping effect of CDSWASL will be obtained.

Key words: damping structure, stand-off layer, complex stiffness method, loss factor

1. Introduction

Constrained damping structure with a stand-off layer (CDSWASL) is constructed by adding a stand-off layer between base layer and damping layer of conventional constrained damping structure, and the material property of the stand-off layer is between damping layer material's and base layer material's. The structure is shown in Fig.1. For the similar lever-enlarge function of the stand-off layer which increasing damping layer's shear deformation and the better damping ability itself, the energy dissipation effect and the rigidity of the whole structure can be improved. Some scholars have done research on CDSWASL: Jessica M. Yellin et al. [1] built a passive constrained four-layer beam model.

¹ Lecturer, PhD candidate, Mechanical Engineering College, Taiyuan University of Science and Technology, China, email: 364795838@qq.com

² Prof., Mechanical Engineering College, Taiyuan University of Science and Technology, China, email: Sundgbox@163.com

³ Associate Prof., Mechanical Engineering College, Taiyuan University of Science and Technology, China, email: 396034241@qq.com

⁴ Lecturer, Mechanical Engineering College, Taiyuan University of Science and Technology, China, email: Lizlbox@163.com

They gave the kinematic equations and verified the results by related tests. Based on FEM and ANSYS, Zhaoyou Wei et al. [2] built a constrained damping beam with a slot stand-off layer and made modal analysis. Huirong Shi et al. [3] optimized the design of constrained damping beam with a stand-off layer under the help of FEM. They analyzed and compared the vibration characteristics between continuous and discontinuous constrained layer. A.W.v Vuure et al. [4] adopted strain energy method to predict the damping effect of multilayer structure. When each layer's material loss factor is known, they could predict the multilayer damping effect by computing the distribution of strain energy with ANSYS. Sanjiv Kumar et al. [5] gave the kinematics equations of constrained damping structure with an active stand-off layer by using Hamilton principle and FEM. Caiyou Zhao et al. [6] applied the stand-off layer to train tracks damping. They built a constrained damping structure model which including a slot stand-off layer and carried out related test. By using simple proportional feedback control strategy, they gave out the numerical solution of complex eigenvalue for kinematics equations.

At present, the methods that are used to solve the structural loss factor are mainly numerical method and FEM. Complex stiffness method (CSM), as a relatively simple and practical numerical analysis method, aroused the concern of some researchers. Tso-Liang teng et al. [7] used the complex stiffness method to analyze and calculate the loss factor of three layers damping laminated beam. Denys J. Mead [8] measured the loss factor of beams and plates with constrained or unconstrained damping layers by using CSM. He regarded the CSM as a critical method to assess the damping effect of a structure. Graig Allen Gsllimore [9] computed the loss factor of the constrained damping device used in the small scale aircraft landing gearing system by CSM and verified the results through experiment. M. L. Aenlle et al. [10] calculated the loss factor of the laminated glass damping structure by CSM and analyzed the effective thickness of laminated glass.

Based on CSM, the formula to calculate the loss factor of CDSWASL is deduced and the influence of geometry, material parameters and laying position for stand-off layer on the loss factor is discussed in the paper.

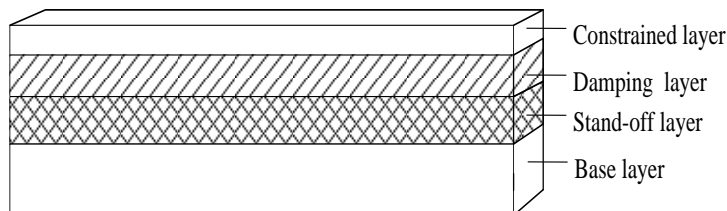


Fig.1 Constrained damping beams with a stand-off layer

2 Theoretical model

2.1 Calculation of complex stiffness for CDSWASL

In the paper, taking constrained damping beam with a stand-off layer as an example, the equation to calculate the complex stiffness for CDSWASL would be deduced. The rectangular coordinate system is set up in Fig 2a. Now, a micro unit of CDSWASL is cut out for analyzing. The deformation of micro unit is showed in Fig 2b. In Fig. 2b, α is the shear angle of constrained layer and base layer, β is the shear angle of stand-off layer and γ is the shear angle of damping layer. H_i ($i=1,2,3,4$) is the thickness of base layer, stand-off layer, damping layer and constrained layer respectively.

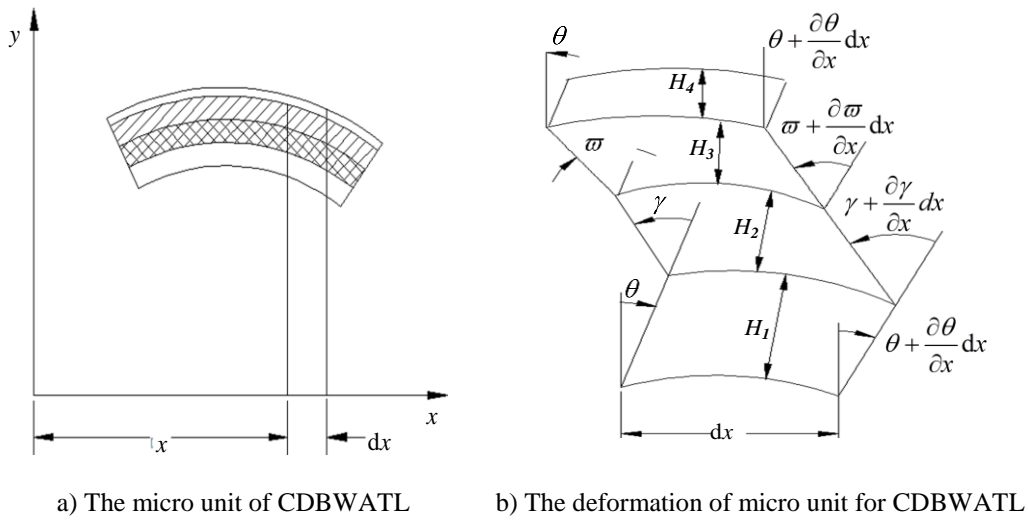


Fig.2 The micro-unit deformation of CDSWASL

The motion differential equation of CDBWATL is showed in the following:

$$B^* \frac{\partial^4 y}{\partial x^4} + m \frac{\partial^2 y}{\partial t^2} = f(x, t) \quad (1)$$

where B^* is the complex bending stiffness of CDBWATL, which can be obtained by the bending moment M . The M can be calculated by the following equation.

$$M = B^* \frac{\partial \alpha}{\partial x} = \sum_{i=1}^4 M_{ii} + \sum_{i=1}^4 F_i H_{i0} \quad (i=1-4) \quad (2)$$

where M_{ii} is i layer's bending moment which generated by i layer relative to its neutral surface. Let K_i^* be the complex tensile stiffness of i layer, M_{ii} can be written as the follows respectively.

$$\left. \begin{aligned} M_{11} &= K_1^* \frac{H_1^2}{12} \times \frac{\partial \alpha}{\partial x} \\ M_{22} &= K_2^* \frac{H_2^2}{12} \left(\frac{\partial \alpha}{\partial x} - \frac{\partial \beta}{\partial x} \right) \\ M_{33} &= K_3^* \frac{H_3^2}{12} \left(\frac{\partial \alpha}{\partial x} - \frac{\partial \beta}{\partial x} - \frac{\partial \gamma}{\partial x} \right) \\ M_{44} &= K_4^* \frac{H_4^2}{12} \bullet \frac{\partial \alpha}{\partial x} \end{aligned} \right\} \quad (3)$$

where H_{i0} is the distance from the neutral plane of i layer to the neutral plane of the whole damping beam which can be seen as 0-0 plane in Fig. 3. F_i is the pure tensile force of i layer respectively, and its expression can be written as the follows.

$$\left. \begin{aligned} F_1 &= K_1^* H_{10} \frac{\partial \alpha}{\partial x} \\ F_2 &= K_2^* \left(H_{20} \frac{\partial \alpha}{\partial x} - \frac{H_2}{2} \frac{\partial \beta}{\partial x} \right) \\ F_3 &= K_3^* \left(H_{30} \frac{\partial \alpha}{\partial x} - H_2 \frac{\partial \beta}{\partial x} - \frac{H_3}{2} \frac{\partial \gamma}{\partial x} \right) \\ F_4 &= K_4^* \left(H_{40} \frac{\partial \alpha}{\partial x} - H_2 \frac{\partial \beta}{\partial x} - H_3 \frac{\partial \gamma}{\partial x} \right) \end{aligned} \right\} \quad (4)$$

From Fig. 3, the follows can be draw.

$$H_{10} = -D; \quad H_{20} = H_{21} - D; \quad H_{30} = H_{31} - D; \quad H_{40} = H_{41} - D \quad (5)$$

To the bending vibration of CDBWATL, according to $\sum_{i=1}^4 F_i = 0$, the neutral surface position D can be obtained.

$$D = \frac{\left(K_2^* H_{21} + K_3^* H_{31} + K_4^* H_{41} \right) - \left(\frac{K_2^*}{2} + K_3^* + K_4^* \right) H_2 \frac{\partial \beta}{\partial \alpha} - \left(\frac{K_3^*}{2} + K_4^* \right) H_3 \frac{\partial \gamma}{\partial \alpha}}{K_1^* + K_2^* + K_3^* + K_4^*} \quad (6)$$

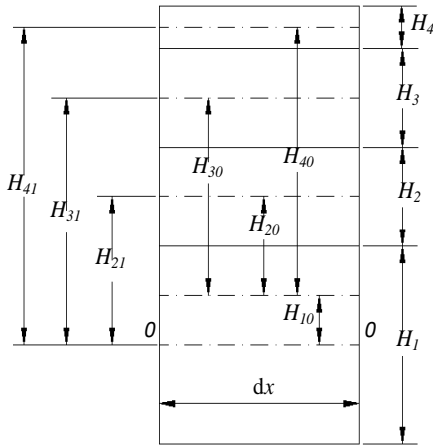


Fig.3 Neutral plane of each layer

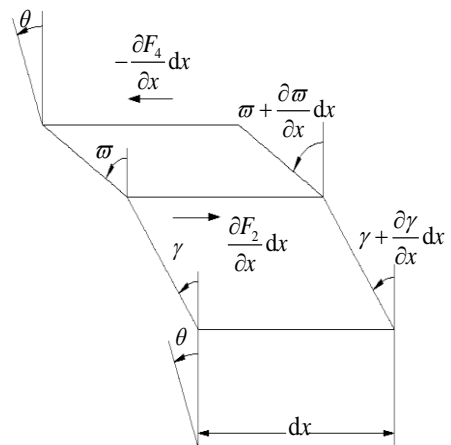


Fig.4 The schematic of shear force balance

When putting Eq. (3), (4), (6) into Eq. (2), the complex stiffness B^* of CDSWASL can be obtained.

$$\begin{aligned} B^* = & K_1^* \frac{H_1^2}{12} + K_2^* \frac{H_2^2}{12} + K_3^* \frac{H_3^2}{12} + K_4^* \frac{H_4^2}{12} + K_1^* D^2 + K_2^* (H_{21} - D)^2 + K_3^* (H_{31} - D)^2 \\ & + K_4^* (H_{41} - D)^2 - \left(K_3^* \frac{H_3^2}{12} + K_3^* \frac{H_3}{2} (H_{31} - D) + K_4^* H_3 (H_{41} - D) \right) \frac{\partial \gamma}{\partial \alpha} \\ & - \left(K_2^* \frac{H_2}{2} (H_{21} - D) + K_3^* \frac{H_3^2}{12} + K_3^* H_2 (H_{31} - D) + K_4^* H_2 (H_{41} - D) + K_2^* \frac{H_2^2}{12} \right) \frac{\partial \beta}{\partial \alpha} \end{aligned} \quad (7)$$

By analyzing Eq. (7), it can be seen that there exists relation between the value of complex stiffness B^* and the shear angle $\frac{\partial \beta}{\partial \alpha}$ and $\frac{\partial \gamma}{\partial \alpha}$ which belong to stand-off layer and base layer and damping layer and stand-off layer respectively.

For the shear force balance showed in Fig. 4, the follows can be obtained.

$$\left. \begin{array}{l} \gamma = -G_3 \frac{\partial F_4}{\partial x} \\ G_3^* \gamma = G_2^* \beta \rightarrow \beta = \frac{G_3^*}{G_2^*} \gamma \\ \frac{\partial^2 \beta}{\partial x^2} = \frac{G_3^*}{G_2^*} \frac{\partial^2 \gamma}{\partial x^2} \end{array} \right\} \quad (8)$$

where G_2^* is the shear parameter of stand-off layer while G_3^* is the damping layer's.

Assuming γ changing like the sine, the following equations can be drawn.

$$\gamma = \gamma_0 \sin px, \quad \frac{\partial^2 \gamma}{\partial x^2} = -p^2 \gamma$$

where p is wave number.

The equation $\frac{\partial^2 \gamma}{\partial x^2} = -p^2 \gamma$ can be changed into the follows.

$$\gamma = -\frac{1}{p^2} \frac{\partial^2 \gamma}{\partial x^2} \quad (9)$$

When substituting Eq. (4) into (8) and making it equal to Eq. (9), the following equation can be drawn.

$$\begin{aligned} -\frac{1}{G_3^*} K_4^* \left((H_{41} - D) \frac{\partial^2 \alpha}{\partial x^2} - H_2 \frac{G_3^*}{G_2^*} \frac{\partial^2 \gamma}{\partial x^2} - H_3 \frac{\partial^2 \gamma}{\partial x^2} \right) &= -\frac{1}{p^2} \frac{\partial^2 \gamma}{\partial x^2} \\ \frac{\partial^2 \gamma}{\partial x^2} &= \frac{H_{41} - D}{\frac{G_3^*}{p^2 K_4^*} + H_2 \frac{G_3^*}{G_2^*} + H_3} \end{aligned} \quad (10)$$

For the sinusoidal changes of γ and α , the equation $\frac{\partial^2 \gamma}{\partial x^2} = \frac{\partial \gamma}{\partial \alpha}$ can be

obtained and the following equation can be drawn.

$$\begin{aligned}\frac{\partial\gamma}{\partial\alpha} &= \frac{H_{41}-D}{\frac{G_3^*}{p^2K_4^*}+H_2\frac{G_3^*}{G_2^*}+H_3} \\ \frac{\partial\beta}{\partial\alpha} &= \frac{H_{41}-D}{\frac{G_2^*}{p^2K_4^*}+H_3\frac{G_2^*}{G_3^*}+H_2}\end{aligned}\quad (11)$$

Substituting Eq. (10) into (6), the following equation can be deduced.

$$D = \frac{H_3 H_{41} g_2 \left(\frac{K_3^*}{2} + K_4^* \right) + H_{41} H_2 g_1 \left(\frac{K_2^*}{2} + K_3^* + K_4^* \right) - g_1 g_2 \left(K_2^* H_{21} + K_3^* H_{31} + K_4^* H_{41} \right)}{H_2 g_1 \left(\frac{K_2^*}{2} + K_3^* + K_4^* \right) + H_3 g_2 \left(\frac{K_3^*}{2} + K_4^* \right) - g_1 g_2 \left(K_1^* + K_2^* + K_3^* + K_4^* \right)} \quad (12)$$

where

$$\begin{aligned}g_1 &= \frac{G_3^*}{p^2 K_4^*} + H_2 \frac{G_3^*}{G_2^*} + H_3 \\ g_2 &= \frac{G_2^*}{p^2 K_4^*} + H_3 \frac{G_2^*}{G_3^*} + H_2\end{aligned}$$

here, p is the wave number, and it can be calculated by the following equation [9].

$$p^2 = \frac{\xi_n^2 \sqrt{C_n}}{L^2}, \xi_n^4 = \frac{\rho_1 b h_1 \omega_n^2 L^4}{E I_1}$$

where ξ_n is n -order damping ratio, ω_n is n -order modal frequency, and C_n is Rao correction factor [11]. The C_n specific value can be seen in table 1.

Table 1.
The Rao correction factors

The boundary conditions	Mode 1	Mode 2 and so on
Clamped on both ends	1	1
Fixed on both ends	1.4	1
One end fixed and one end simply supported	1	1
One end fixed and one end free	0.9	1
Both ends free	1	1

When substituting Eq. (12) into (11), Eq. (11) can be changed into the following.

$$\frac{\partial \beta}{\partial \alpha} = \frac{g_1 \left(K_2^* (H_{21} - H_{41}) + K_3^* K_{31} - K_1^* H_{41} - K_3^* H_{41} \right)}{g_2 H_3 \left(K_4^* + \frac{K_3^*}{2} \right) + g_1 H_2 \left(\frac{K_2^*}{2} + K_3^* + K_4^* \right) - g_1 g_2 \left(K_1^* + K_2^* + K_3^* + K_4^* \right)} \quad (13)$$

$$\frac{\partial \gamma}{\partial \alpha} = \frac{g_2 \left(K_2^* (H_{21} - H_{41}) + K_3^* H_{31} - K_1^* H_{41} - K_3^* H_{41} \right)}{g_2 H_3 \left(K_4^* + \frac{K_3^*}{2} \right) + g_1 H_2 \left(\frac{K_2^*}{2} + K_3^* + K_4^* \right) - g_1 g_2 \left(K_1^* + K_2^* + K_3^* + K_4^* \right)}$$

For $K_3^* \ll K_1^*$, K_3^* can be ignored and omitted. Eq. (11) and (12) would be changed into the following forms.

$$D = \frac{H_3 H_{41} g_2 K_4^* + H_{41} H_2 g_1 \left(\frac{K_2^*}{2} + K_4^* \right) - g_1 g_2 \left(K_2^* H_{21} + K_4^* H_{41} \right)}{H_2 g_1 \left(\frac{K_2^*}{2} + K_4^* \right) + H_3 g_2 K_4^* - g_1 g_2 \left(K_1^* + K_2^* + K_4^* \right)} \quad (14)$$

$$\frac{\partial \beta}{\partial \alpha} = \frac{g_1 \left(K_2^* (H_{21} - H_{41}) - K_1^* H_{41} \right)}{g_2 H_3 K_4^* + g_1 H_2 \left(\frac{K_2^*}{2} + K_4^* \right) - g_1 g_2 \left(K_1^* + K_2^* + K_4^* \right)} \quad (15)$$

$$\frac{\partial \gamma}{\partial \alpha} = \frac{g_2 \left(K_2^* (H_{21} - H_{41}) - K_1^* H_{41} \right)}{g_2 H_3 K_4^* + g_1 H_2 \left(\frac{K_2^*}{2} + K_4^* \right) - g_1 g_2 \left(K_1^* + K_2^* + K_4^* \right)}$$

Substituting Eq. (14) (15) into (7), the complex stiffness of can be drawn.

$$B^* \approx x1 + x2 + x3 + \frac{K_1^* H_1^2}{12} + \frac{K_2^* H_2^2}{12} + \frac{K_3^* H_3^2}{12} + \frac{K_4^* H_4^2}{12} + K_1^* \frac{a^2}{b^2} \quad (16)$$

where

$$\begin{aligned}
x1 &= K_2^* \left(H_{21} - \frac{a}{b} \right)^2 + K_3^* \left(H_{31} - \frac{a}{b} \right)^2 + K_4^* \left(H_{41} - \frac{a}{b} \right)^2 \\
x2 &= \frac{g_1 c \left(K_2^* \frac{H_2^2}{12} + K_3^* \frac{H_3^2}{12} + K_2^* \frac{H_2}{2} \left(H_{21} - \frac{a}{b} \right) + K_3^* H_2 \left(H_{31} - \frac{a}{b} \right) + K_4^* H_2 \left(H_{41} - \frac{a}{b} \right) \right)}{b} \\
x3 &= \frac{g_2 c \left(\frac{K_3^* H_3^2}{12} + \frac{K_3^*}{2} H_3 \left(H_{31} - \frac{a}{b} \right) + K_4^* H_3 \left(H_{41} - \frac{a}{b} \right) \right)}{b} \\
a &= g_2 K_4^* H_2 H_{41} - g_1 g_2 \left(K_2^* H_{21} + K_4^* H_{41} \right) + g_1 H_{41} \left(\frac{K_2^*}{2} + K_4^* \right) \\
b &= g_2 K_4^* H_3 + g_1 H_2 \left(K_2^* + K_4^* \right) - g_1 g_2 \left(K_1^* + K_2^* + K_4^* \right) \\
c &= K_1^* H_{41} - K_2^* \left(H_{21} - H_{41} \right)
\end{aligned}$$

2.2 Calculation of structural loss factor

Using equation (16), the loss factor of CDSWASL can be obtained by the follows

$$\eta = \frac{\text{Im}(B^*)}{\text{Re}(B^*)} \quad (17)$$

3. Model validation

In order to verify the correctness of Eq. (17), the following CDSWASL model is built. The parameters are: $L=0.3\text{m}$, $b=0.04\text{m}$, $H_1=0.005\text{m}$, $E_1=207\times10^9\text{pa}$, $\mu_1=0.3$, $\rho_1=7850\text{kg/m}^3$; $H_2=0.0025\text{m}$, $G_2=5.28\times10^8(1+0.3825i)\text{pa}$, $\mu_2=0.35$, $\rho_2=1500\text{kg/m}^3$; $H_3=0.003\text{m}$, $G_3=2.615\times10^5(1+0.9683i)\text{pa}$, $\mu_3=0.49$, $\rho_3=999\text{kg/m}^3$; $H_4=0.005\text{m}$, $E_1=207\times10^9\text{pa}$, $\mu_4=0.3$, $\rho_1=7850\text{kg/m}^3$.

Table.2

The comparison between CSM and FEM

Mode	Loss factor		
	CSM	FEM	Error %
1	0.1809	0.2025	8.2%
2	0.0905	0.0985	8.8%
3	0.0681	0.0755	7.9%
4	0.0613	0.0721	9.3%

Using CSM and FEM to calculate the structural loss factor respectively, the results are shown in table 2.

From table 2, it can be seen that the errors between the results computing by CSM and FEM are less than 10%. So, it is reliable for using CSM to compute the structural loss factor.

4. The comparison between CDSWASL and TCDS

The properties of the cantilever beam are: $L=0.15\text{m}$, $b=0.1175\text{m}$, $H_1=0.00229\text{m}$, $E_1=72\times 10^9\text{pa}$, $\mu_1=0.3$, $\rho_1=2850\text{kg/m}^3$, $H_3=0.002767\text{m}$, $G_3=1\times 10^5(1+i)\text{pa}$, $\mu_3=0.45$, $\rho_3=999\text{kg/m}^3$, $H_4=0.000127\text{m}$, $E_4=207\times 10^9\text{pa}$, $\mu_4=0.3$, $\rho_4=7850\text{kg/m}^3$.

Taking the following three models to compared: 1) TCDS. The damping layer thickness is: $H_3=0.002767\text{m}$; 2) TCDS. Increasing the damping layer thickness, the thickness of damping layer is: $H_3=0.003767$; 3) CDSWASL. Adding a stand-off layer between base layer and damping layer, the parameters of stand-off layer are: $H_2=0.001\text{m}$, $G_2=5\times 10^8(1+0.38i)\text{pa}$.

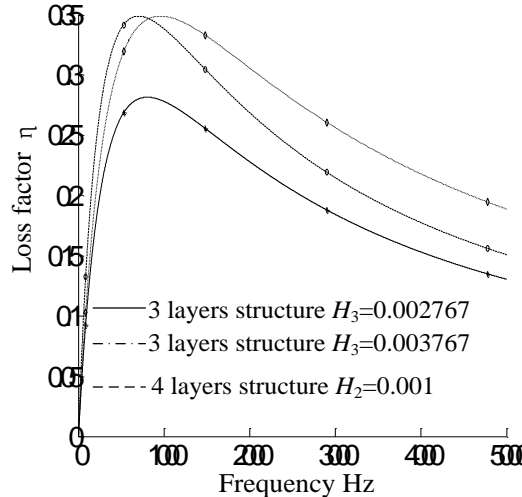


Fig.5 The comparison of loss factor between CDSWASL and TCDS

The comparison curves of loss factor for three models are shown in Fig. 5. From Fig. 5, it can be seen that the loss factor of model 3 is significantly higher than that of model 1. The reason is that the stand-off layer can lever the deformation of damping layer to make the model 3 have a better damping effect than model 1. Additionally, it also can be seen that the loss factor of model 3 is significantly higher than that of model 2 except the low frequency phase, which means the deformation of damping layer increasing in model 3 by the levering effect of stand-off layer is more than that in model 2 by adding the thickness of damping layer. Through the analysis above, the conclusion can be drawn that: the damping effect can be improved by increasing the damping layer thickness or adding stand-off layer between base layer and damping layer. In contrast to

increasing the damping layer thickness to improve the damping effect, adding stand-off layer is the better way for it not only increasing the shear deformation of damping layer more to improve the structural damping effect but also improving the whole structural stiffness.

5. Parameters analysis of stand-off layer

5.1 Material properties of stand-off layer

The parameters of the cantilever model are the follows: $L=0.15\text{m}$, $b=0.00175\text{m}$, $H_1=0.00229\text{m}$, $\rho_1=7850\text{kg/m}^3$, $E_1=207\times10^9\text{pa}$, $H_2=0.001\text{m}$, $H_3=0.002767\text{m}$, $G_3=10^5\times(1+0.9i)\text{pa}$, $H_4=0.000203\text{m}$, $E_4=207\times10^9\text{pa}$, $\rho_4=7850\text{ kg/m}^3$.

Since the deformation of damping layer is mainly shear deformation in constrained damping structure, the size of the structural loss factor is related to the shear deformation of the damping layer. After adding the stand-off layer, the stand-off layer can increase the deformation of damping layer and improve the damping effect when the structure deforming. When using four types material which having different shear modulus and loss factor as the stand-off layer respectively, the structural loss factors change trends can be seen in Fig. 6.

From Fig. 6, it can be seen that there exist the following relations between the structural loss factor and shear modulus and loss factor of the material for stand-off layer.

(1) When material of stand-off layer is relatively soft ($E_2/E_3 < 1000$), the material properties of stand-off layer and damping layer almost are the same, and the located stand-off layer is only added the thickness of damping layer, so the material of stand-off layer has little effect on structural loss factor.

(2) When material of stand-off layer is relatively hard ($E_2/E_3 > 1000$), the loss factor of stand-off layer has a greater impact on structural loss factor.

i) If the loss factor of stand-off layer is small such as $\beta=0.0125$ and $\beta=0.0312$, the structural loss factor would decrease with the shear modulus of stand-off layer increasing. The reason is: when the material of stand-off layer has a very small loss factor and enough hard shear modulus, its material property approximates to that of metal material, so the effect of stand-off layer is only to increase the stiffness of base layer which make the deformation of damping layer decease.

ii) If the loss factor of stand-off layer is large such as $\beta=0.531$ or $\beta=0.824$, the loss factor of the structure would increase and then decrease with the increasing of the shear modulus of material. The reason why occurs above trends is that: when the stand-off layer has a higher loss factor and enough shear modulus, its lever effect can reach the best. But with the shear modulus increasing further, the lever effect would decrease.

From analysis above, it can be drawn that the ideal stand-off layer material should have an infinite shear modulus, an infinitely small flexural modulus and as a large loss factor as possible. However, to actual material for the general, the relations between elastic modulus and loss factor is that the greater the elastic modulus is, the smaller the loss factor is. For examples, the material of base layer generally has large elastic modulus and negligible loss factor while the material of damping layer generally has small elastic modulus and large loss factor. Additionally, it also can be drawn from Fig. 6 that, to make the structural loss factor changing obviously, the elastic modulus of stand-off layer material should be at 1000 times of the elastic modulus of damping layer, and the loss factor of stand-off layer material should be larger as possible.

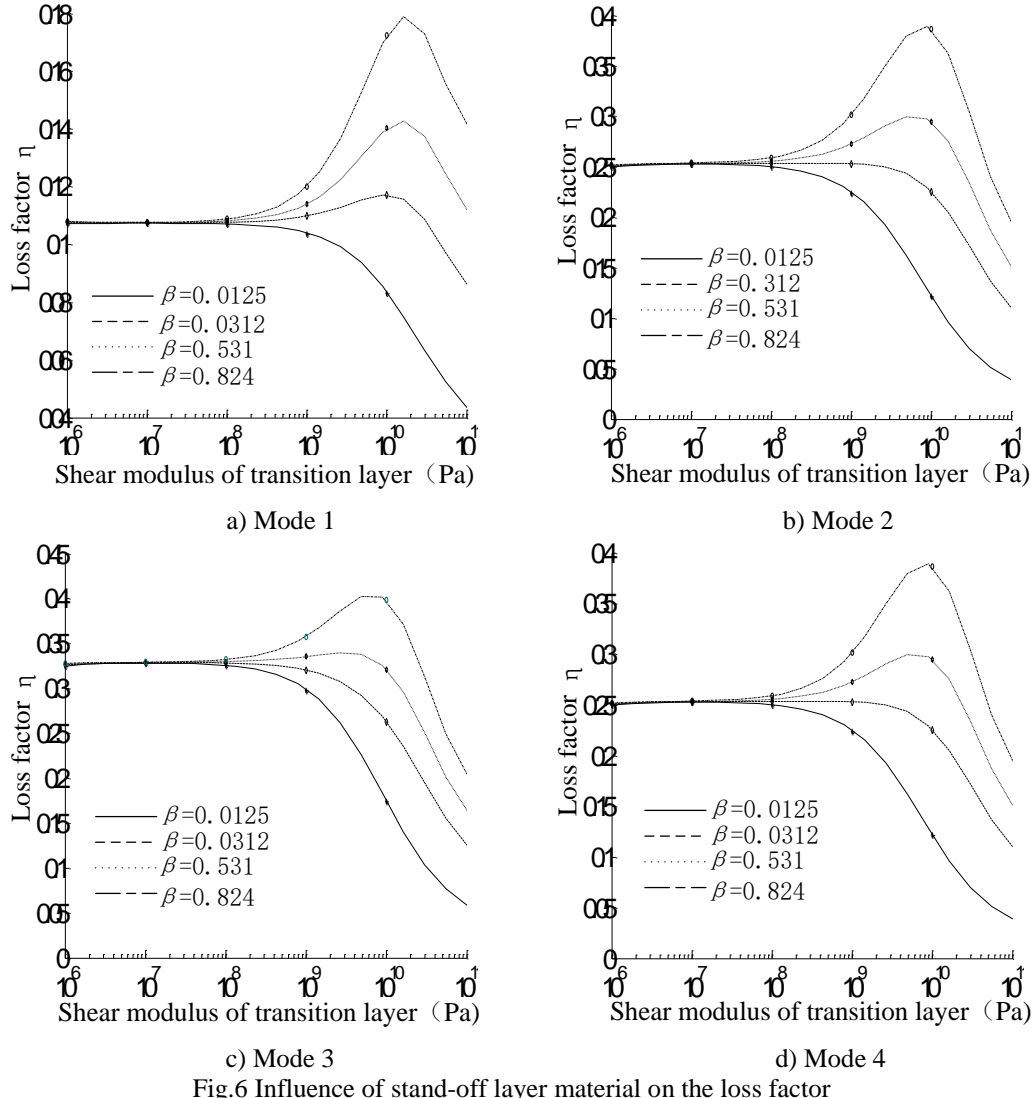


Fig.6 Influence of stand-off layer material on the loss factor

5.2 The thickness analyzing of stand-off layer

The thickness of stand-off layer is 0.001m, 0.002m, 0.003m and 0.004m respectively. The shear modulus of stand-off layer is $5 \times 10^7(1+0.6i)$. The relation between the thickness of stand-off layer and structural loss factor is showed in Fig. 7. From Fig. 7, it can be seen that, with the thickness increasing of stand-off layer, the model loss factor of structure would increase obviously. The reason is that, with the thickness of stand-off layer increasing, the distance between base layer and damping layer is expanded. So, the lever effect of the stand-off layer is more obvious than before. So, under the premise of satisfying the structural size and quality constraint, the structural loss factor can be increased by increasing the thickness of stand-off layer.

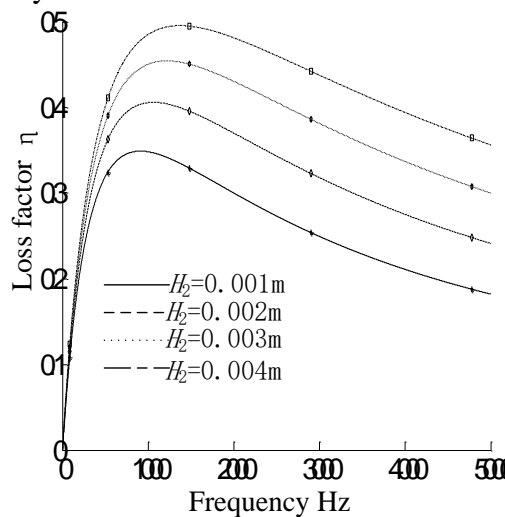


Fig.7 The influence on structure loss factor for the thickness parameter of stand-off damping layer

6. Conclusion

Based on the complex stiffness method, the loss factor of CDSWASL is derived in the paper. Through contrast to add the thickness of damping layer to improve the structure damping effect, the CDSWASL is the more effective way for it not only increasing the shear deformation of damping layer to improve the structural damping effect but also improving the whole structural stiffness. By the parameter analysis of stand-off layer, the following conclusion can be drawn.

(1) The material of stand-off layer can play a great role on the structure damping effect. When the ratio of elastic modulus between the stand-off layer and damping layer is at 1000 and the stand-off layer material has a certain loss factor, the best structure damping effect can be obtained.

(2) The thickness of stand-off layer also has a great impact on the structure damping effect. The thicker stand-off layer is, the greater levering effect it can

play to increasing the deformation of damping layer. So, on the premise of satisfying the structural size and quality constraint, the structure damping effect can have improved by increasing the thickness of stand-off layer.

Acknowledgement

The work is founded by National Natural Science Foundation of China (51405323) and the TYUST Foundation for Doctor (20162005, 20162035).

R E F E R E N C E S

- [1] *J.M.Yellin, I.Y.Shen and P.G.Reinhall*, “An analytical and experimental analysis for a one-dimensional passive stand-off layer damping treatment”, in *Journal of Vibration and Acoustics*, **vol. 122**, no. 4, Oct. 2000, pp. 440-447
- [2] *R.S.Mastic and M.,G.Sainsbury*, “Vibration damping of cylindrical shells partially coated with a constrained viscoelastic treatment having a standoff layer”, in *Thin-Walled Structures*, **vol. 43**, no. 9, Sep. 2005, pp. 1355-1379
- [3] *H.R.Shi and D.Y.Zhao*, “Reducing vibration and optimization design of beam with a stand-off constrained layer damping patch”, in *Journal of Machine Design*, **vol. 27**, no. 12, Dec. 2010, pp. 79-84
- [4] *A.W.V.Vuure, I.Verpoest and F.K.Ko*, “Sandwich-fabric panels as spacers in a constrained layer structural damping application”, in *Composites Part B Engineering*, **vol. 32**, no. 1, Jan. 2001, pp. 11-19
- [5] *S.Kumar, R.Kumar and R.Sehgal*, “Enhanced ACLD treatment using stand-off-layer: FEM based design and experimental vibration analysis”, in *Applied Acoustics*, **vol. 72**, no. 11, Nov. 2011, pp. 856-872
- [6] *C.Y.Zhao and P.Wang*, “Theoretical Modelling and Effectiveness Study of Slotted Stand-Off Layer Damping Treatment for Rail Vibration and Noise Control”, in *Shock & Vibration*, **vol. 15**, no. 3, Jan. 2015, pp. 1-12
- [7] *T.L.Teng and N.K.Hu*, “Analysis of damping characteristics for viscoelastic laminated beams”, in *Computer Methods in Applied Mechanics & Engineering*, **vol. 190**, no. 29-30, Apr. 2001, pp. 3881-3892
- [8] *D.J.Mead*, “The measurement of the loss factors of beams and plates with constrained and unconstrained damping layers: A critical assessment”, in *Journal of Sound & Vibration*, **vol. 300**, no. 3-5, Mar. 2007, pp. 744-762
- [9] *C.A.Gallimore*, Passive Viscoelastic Constrained Layer Damping Application for a Small Aircraft Landing Gear System, B.S. Thesis, The Virginia Polytechnic Institute and State University, 2008
- [10] *M.L.Aenlle*, “Frequency Response of Laminated Glass Elements: Analytical Modeling and Effective Thickness”, in *Applied Mechanics Reviews*, **vol. 65**, no. 2, Apr. 2013, pp. 1388-1404
- [11] *D.I.G.Jones*, Handbook of viscoelastic vibration damping, England: John Wiley and Sons, LTD, West Sussex, 2001